AEM
Journals.ASM.org

Metabolism of Doubly *para*-Substituted Hydroxychlorobiphenyls by Bacterial Biphenyl Dioxygenases

Thi Thanh My Pham,[a] Mohammad Sondossi,[b] Michel Sylvestre[a]

Institut National de la Recherche Scientifique, INRS—Institut Armand-Frappier, Laval, QC, Canada[a]; Department of Microbiology, Weber State University, Ogden, Utah, USA[b]

In this work, we examined the profile of metabolites produced from the doubly *para*-substituted biphenyl analogs 4,4′-dihydroxybiphenyl, 4-hydroxy-4′-chlorobiphenyl, 3-hydroxy-4,4′-dichlorobiphenyl, and 3,3′-dihydroxy-4,4′-chlorobiphenyl by biphenyl-induced *Pandoraea pnomenusa* B356 and by its biphenyl dioxygenase (BPDO). 4-Hydroxy-4′-chlorobiphenyl was hydroxylated principally through a 2,3-dioxygenation of the hydroxylated ring to generate 2,3-dihydro-2,3,4-trihydroxy-4′-chlorobiphenyl and 3,4-dihydroxy-4′-chlorobiphenyl after the removal of water. The former was further oxidized by the biphenyl dioxygenase to produce ultimately 3,4,5-trihydroxy-4′-chlorobiphenyl, a dead-end metabolite. 3-Hydroxy-4,4′-dichlorobiphenyl was oxygenated on both rings. Hydroxylation of the nonhydroxylated ring generated 2,3,3′-trihydroxy-4′-chlorobiphenyl with concomitant dechlorination, and 2,3,3′-trihydroxy-4′-chlorobiphenyl was ultimately metabolized to 2-hydroxy-4-chlorobenzoate, but hydroxylation of the hydroxylated ring generated dead-end metabolites. 3,3′-Dihydroxy-4,4′-dichlorobiphenyl was principally metabolized through a 2,3-dioxygenation to generate 2,3-dihydro-2,3,3′-trihydroxy-4,4′-dichlorobiphenyl, which was ultimately converted to 3-hydroxy-4-chlorobenzoate. Similar metabolites were produced when the biphenyl dioxygenase of *Burkholderia xenovorans* LB400 was used to catalyze the reactions, except that for the three substrates used, the BPDO of LB400 was less efficient than that of B356, and unlike that of B356, it was unable to further oxidize the initial reaction products. Together the data show that BPDO oxidation of doubly *para*-substituted hydroxychlorobiphenyls may generate nonnegligible amounts of dead-end metabolites. Therefore, biphenyl dioxygenase could produce metabolites other than those expected, corresponding to dihydrodihydroxy metabolites from initial doubly *para*-substituted substrates. This finding shows that a clear picture of the fate of polychlorinated biphenyls in contaminated sites will require more insights into the bacterial metabolism of hydroxychlorobiphenyls and the chemistry of the dihydrodihydroxylated metabolites derived from them.

The toxicity of hydroxybiphenyls in antimicrobial preparations used as biocides has been exploited for many years (1). In addition, hydroxybiphenyls are key intermediates produced from multiple sources. For example, they are produced from the microbial metabolism of dibenzofuran, fluorene, and carbazole (2, 3). In polychlorinated biphenyl (PCB)-contaminated sites, hydroxychlorobiphenyls are generated by the bacterial biphenyl catabolic enzymes (4) and by plant enzymatic systems (5, 6). In addition, hydroxychlorobiphenyls may be produced in significant amounts by abiotic processes (7). The presence of these hydroxylated metabolites in the environment may impact the ecosystems in which they are generated since they are toxic to living organisms, including bacteria (8). Among their toxicological effects toward mammals, certain congeners are recognized endocrine disrupters (7). Because of the numerous concerns about their environmental impacts, hydroxychlorobiphenyls are increasingly considered a new class of environmental contaminants (for a complete review about the sources of production and the toxicity of hydroxychlorobiphenyls, see the report by Tehrani and Van Aken [9]). However, their fate in the environment has been scarcely investigated. The pathway used by aerobic bacteria to degrade biphenyl is also used to metabolize or cometabolize several hydroxy- and hydroxychlorobiphenyls with an initial attack by the biphenyl dioxygenase (BPDO) (9). However, the profile of the metabolites generated by this pathway has been determined for only a few of these biphenyl analogs (8, 10, 11). The metabolism of an *ortho*-hydroxylated biphenyl by a monooxygenase has also been reported. The hydroxybiphenyl-degrading *Pseudomonas* sp. strain HBP1 and its 2-hydroxybiphenyl 3-monooxygenase have been well characterized (12).

The biphenyl catabolic pathway is composed of the four enzymatic steps shown in Fig. 1. The oxygenase component (BphAE) of the biphenyl dioxygenase initiates the metabolism by insertion of molecular oxygen onto vicinal *ortho-meta* carbons to generate the *cis*-2,3-dihydro-2,3-dihydroxybiphenyl, which is then oxidized to a catechol and cleaved. The encoding genes in *Pandoraea pnomenusa* B356 are *bphAE* for the oxygenase component and *bphFG* for the ferredoxin (BphF) and reductase (BphG) components of the biphenyl dioxygenase and *bphBCD* for the 2,3-dihydro-2,3-dihydroxybiphenyl dehydrogenase (BphB), the 2,3-dihydroxybiphenyl 1,2-dioxygenase (BphC), and the 2-hydroxy-6-oxo-6-phenylhexa-2,4-dienoic acid (HODA) hydrolase (BphD) (Fig. 1). The enzymes of the biphenyl catabolic pathway are very versatile. Beside PCBs they may also metabolize diphenylmethane as well as heterocyclic aromatics, including dibenzofuran, quino-

Received 10 March 2015 **Accepted** 6 May 2015
Accepted manuscript posted online 8 May 2015
Citation Pham TTM, Sondossi M, Sylvestre M. 2015. Metabolism of doubly *para*-substituted hydroxychlorobiphenyls by bacterial biphenyl dioxygenases. Appl Environ Microbiol 81:4860–4872. doi:10.1128/AEM.00786-15.
Editor: R. E. Parales
Address correspondence to Michel Sylvestre, Michel.Sylvestre@iaf.inrs.ca.

doi:10.1128/AEM.00786-15

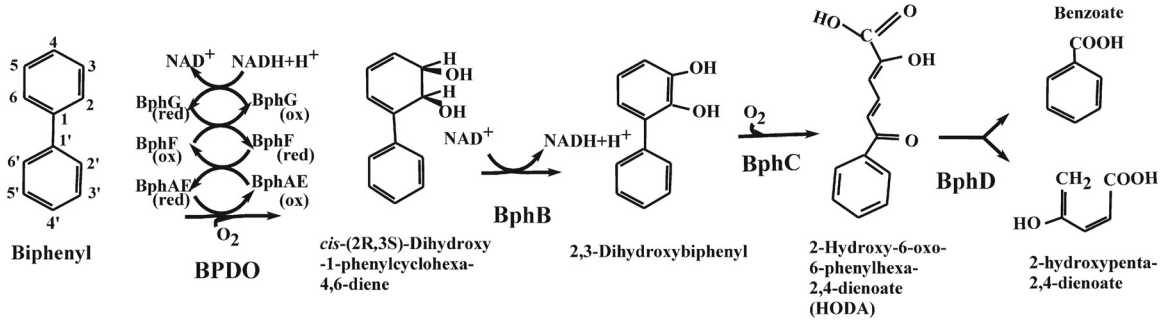

FIG 1 The four enzymatic steps of the bacterial biphenyl catabolic pathway. red, reduction; ox, oxidation.

line, and many phenolics, such as flavonoids derived from plants (2, 8, 10, 13–16).

The specificity of the BPDO is crucial to determine the range of biphenyl analogs metabolized by the biphenyl catabolic pathway. For this reason, significant effort has been invested to characterize this enzyme, and the three-dimensional structure of the oxygenase component (BphAE) of the BPDOs of strain B356 and of *Burkholderia xenovorans* LB400 has been resolved (17, 18). It is now well established that the range of biphenyl analogs metabolized by B356 and LB400 BPDOs differs considerably. Although *B. xenovorans* LB400 is considered to be the best PCB-degrading bacterium that occurs naturally, recent reports have shown that BphAE of strain B356 ($BphAE_{B356}$) metabolizes many biphenyl analogs significantly more efficiently than BphAE of strain LB400 ($BphAE_{LB400}$) (13, 19–21).

It has clearly been established that bacterial BPDOs oxidize chlorinated biphenyls principally on the least substituted or nonsubstituted ring (4). In the case of plants, using *in vitro* plant cells cultures, Kucerova et al. (22) have shown that 4-chlorobiphenyl is hydroxylated onto the 4′-carbon and Rezek et al. (6) have shown that the least substituted ring is the one that is the most often hydroxylated. Fungi were also reported to generate *para*-hydroxylated metabolites of PCBs (23). Although the prevalence of the doubly *para*-hydroxychlorobiphenyls has not been determined precisely, 4-hydroxy-4′-chlorobiphenyl may cause inhibition of state 3 respiration of mitochondria (24), and in addition, several *para*-hydroxychlorobiphenyls were shown to be endocrine disrupters (25). The profiles of metabolites generated from 2,2′- and 3,3′-dihydroxybiphenyl by biphenyl-induced cells of strain B356 were determined in a previous study (8). The ability of the biphenyl catabolic pathway of *B. xenovorans* LB400 to metabolize 4-hydroxy-4′-chlorobiphenyl has recently been demonstrated (16), but the profile of the metabolites produced from doubly *para*-substituted hydroxy- or hydroxychlorobiphenyls has never been reported. In this work, we determined the profile of metabolites produced from selected doubly *para*-substituted hydroxychlorobiphenyls by the biphenyl catabolic pathway enzymes of B356 and LB400. Since many metabolites differed from those expected for a 2,3-dioxygenation of the substrate, to explain their production, we have examined in more detail the catalytic reaction of *P. pnomenusa* B356 and *B. xenovorans* LB400 BPDOs toward these biphenyl analogs. Our data show that BPDO catalytic oxidation of doubly *para*-substituted biphenyl analogs may lead to the production of metabolites other than the expected dihydrodihydroxybiphenyls, many of which are dead-end metabolites that may accumulate in the environment.

MATERIALS AND METHODS

Bacterial strains, plasmids, chemicals, and general protocols. Wild-type strains *P. pnomenusa* B356, *Escherichia coli* DH11S(pDB31 LB400 *bphFG*) (pQE31 B356 *bphAE*), and *E. coli* DH11S(pDB31 LB400 *bphFG*) (pQE31 LB400 *bphAE*), in which pDB31 carries the LB400 *bphFG* genes and pQE31 carries the B356 or LB400 *bphAE* genes, were described previously (20, 26, 27). These two *E. coli* strains express an active BPDO exhibiting the biochemical features of B356 and LB400 BPDOs, respectively. The culture media used were Luria-Bertani (LB) broth (28), M9 basal medium (28), or minimal mineral medium no. 30 (MM30) (29) amended with various sources of carbon and antibiotics, depending on the experiment. 4,4′-Dihydroxybiphenyl, 4-chlorobenzoate, and 4-hydroxybenzoate (99% pure) were from Sigma-Aldrich; 4-chlorobiphenyl, 4,4′-dichlorobiphenyl, 4-hydroxy-4′-chlorobiphenyl, 3-hydroxy-4,4′-dichlorobiphenyl, and 3,3′-dihydroxy-4,4′-dichlorobiphenyl (99% pure) were from Ultra Scientific. Gas chromatography (GC)-mass spectrometry (MS) analyses of these compounds did not reveal any contaminants, such as other hydroxychlorobiphenyls, that may have interfered with the analysis of the profiles of metabolites derived from them.

Whole-cell assays to assess metabolism of the various hydroxychlorobiphenyls by biphenyl catabolic pathway enzymes. Strain B356 was grown at 28°C on MM30 plus biphenyl to reach log phase. Cultures were filtered through packed glass wool to remove particulates, cell aggregates, and crystals of biphenyl. Cells were harvested by centrifugation, washed with phosphate buffer (30 mM, pH 7.2) or M9 medium, and suspended to an optical density at 600 nm (OD_{600}) of 2.0 in MM30 plus the appropriate substrate (27). The suspensions were incubated at 28°C and 100 rpm. After periods varying from 1 to 18 h, depending on the experiments, the cell suspensions were extracted at neutral and acidic pH with ethyl acetate, and the extracts were treated with *N*,*O*-*bis*-trimethylsilyl trifluoroacetamide (TMS) for GC-MS analysis according to previously described protocols (30). GC-MS analyses were performed as described previously (20), using a Hewlett Packard HP6980 series gas chromatograph interfaced with an HP5973 mass selective detector (Agilent Technologies).

Similar whole-cell assays were performed with *E. coli* cells producing the B356 or LB400 BPDO. In this case, *E. coli* DH11S(pDB31 LB400 *bphFG*)(pQE31 B356 *bphAE*) and *E. coli* DH11S(pDB31 LB400 *bphFG*) (pQE31 LB400 *bphAE*) were grown at 37°C to log phase in LB broth with appropriate antibiotics. The cultures were induced for 4 h with 0.5 mM isopropyl-β-D-thiogalactoside (IPTG) and then washed and suspended to an OD_{600} of 2.0 in M9 medium or to an OD_{600} of 5.0 in 50 mM sodium phosphate buffer, pH 7.0, depending on the experiments. The resting cell suspensions were incubated at 37°C for periods varying from 30 min to 18 h with the appropriate hydroxychlorobiphenyls at concentrations ranging from 0.5 to 2 mM. The metabolites were then extracted for GC-MS analyses using protocols identical to the ones described above. Parallel controls were also performed using 4-chlorobiphenyl as the substrate to confirm that the dioxygenase activity was in the same range for both recombinant *E. coli* clones expressing the B356 or LB400 BPDO.

We also assessed the ability of reconstituted His-tagged BPDO prepa-

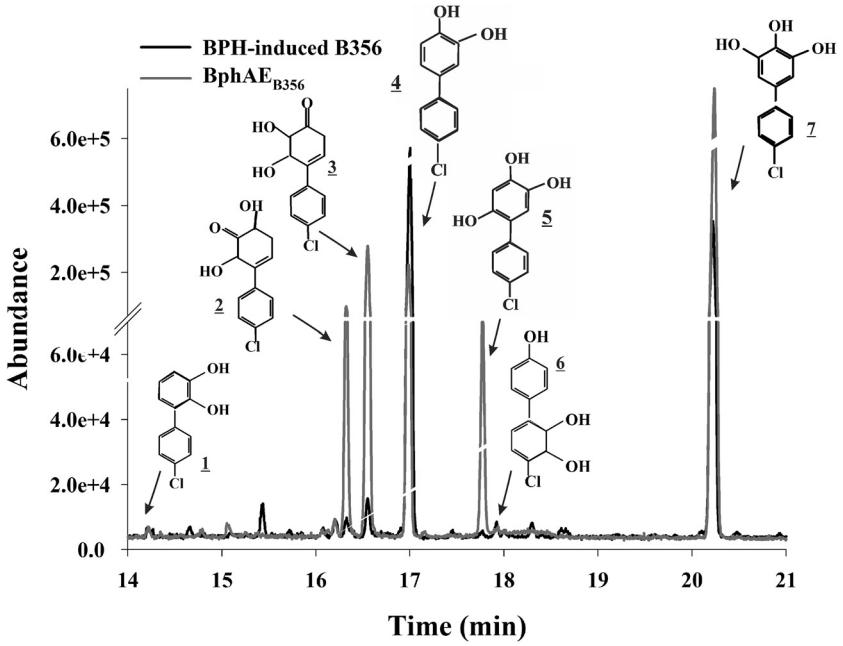

FIG 2 Total ion chromatogram of TMS derivatives of the metabolites produced from 4-hydroxy-4′-chlorobiphenyl by biphenyl (BPH)-induced cells of strain B356 incubated for 90 min with the substrate, as indicated in Materials and Methods (black line), or by a purified preparation of B356 BPDO incubated for 7 min with the substrate (gray line). The metabolite numbering is the same as that in the text and in Table 1. Structures are those of the nonderivatized metabolites.

rations to metabolize hydroxychlorobiphenyls. His-tagged enzyme components were produced and purified by affinity chromatography according to a previously published protocol (31). This protocol produces consistent highly purified enzyme preparations, and the purity of each preparation was assessed by SDS-PAGE. The enzyme assays, in which the assay mixtures contained from 100 to 800 nmol substrate and 1.2 nmol of each enzyme component, were performed in a volume of 200 μl in 50 mM morpholineethanesulfonic acid (MES) buffer, pH 6.0, at 37°C as described previously (32). The reaction medium was incubated for 5 to 15 min, and the metabolites were extracted at pH 6.0 with ethyl acetate and then treated with TMS as described above for GC-MS analysis.

Purification and NMR analysis of 3,4-dihydroxy-4′-chlorobiphenyl, 3,4,5-trihydroxy-4′-chlorobiphenyl, and 4-(4-chlorophenyl)-*cis*-5,6-dihydroxycyclohex-3-en-1-one. 4-Hydroxy-4′-chlorobiphenyl metabolites were produced by use of a reconstituted His-tagged purified preparation of B356 BPDO comprised of BphAEFG from strain B356. The reaction mixture for each enzyme reaction, performed as described above, contained 800 nmol 4-hydroxy-4′-chlorobiphenyl, and the mixture was incubated for 15 min at 37°C. The ethyl acetate extract was concentrated 20-fold by evaporation under a stream of nitrogen, and this preparation was injected into a XDB-C_8 column (4.6 × 150 mm). The high-pressure liquid chromatography (HPLC) conditions were identical to those used in a previous study (20) to purify the benzophenone metabolites produced by purified B356 BPDO preparations. The identity and purity of the eluted metabolites were confirmed by GC-MS analysis of TMS derivatives before running the nuclear magnetic resonance (NMR) analysis. The NMR spectra were obtained at the Quebec/Eastern Canada High Field NMR Facility at McGill University (Montreal, Quebec, Canada) with a Bruker 500-mHz spectrometer. The analyses were carried out in deuterated acetone at room temperature.

Docking and structure analysis. After removal of the cocrystallized ligands and water, dimer AB of BphAE$_{B356}$ (RCSB Protein Data Bank accession number 3GZX) was used as the docking target. Ligand was downloaded as SDF files from PubChem (http://pubchem.ncbi.nlm.nih.gov) and converted into PDB format in the Discover Studio Visualizer (version 2.5) program. In the AutoDockTools program, the ligand was randomly placed into the active site near the mononuclear iron as the starting position. Atomic energy maps were calculated for all types of atoms in the ligand, and the grid map was centered on mononuclear iron and contained 20 points in each *x*, *y*, and *z* direction with the default spacing of 0.375 Å. Then, automatic docking was implemented in the AutoDock (version 4.2) program (33) with the Lamarckian genetic algorithm (LGA) as the search method. The number of LGA runs was increased to produce 20 docking results for further structural analysis.

RESULTS

Analysis of metabolites produced from 4-hydroxy-4′-chlorobiphenyl by purified B356 BPDO. When a purified preparation of B356 BPDO was used to metabolize 4-hydroxy-4′-chlorobiphenyl, several metabolites were produced, but one of them, metabolite 7, was by far the major one. Figure 2 shows the metabolite profile obtained after 7 min of incubation. The fact that the metabolite profile did not vary significantly for incubation times of between 2 min and 15 min suggested that multiple pathways were occurring simultaneously for oxidation of this substrate. On the basis of previous reports (8, 34), the mass spectral features of metabolite 7 (Table 1) corresponded to those of a trihydroxychlorobiphenyl {M^+ at *m/z* 452 and fragmentation ions at *m/z* 437 ($M^+ - CH_3$), 417 ($M^+ - Cl$), 379 [$M^+ - (CH_3)_3Si$], 364 [$M^+ - (CH_3)_4Si$], 349 [$M^+ - (CH_3)_4Si - CH_3$}. Among the minor metabolites, metabolite 1 (Fig. 2) exhibited spectral features that were identical to those of authentic 2,3-dihydroxy-4′-chlorobiphenyl, which is produced from 4-chlorobiphenyl (34). The mass spectral features of metabolite 2 (Table 1) were similar to those of metabolite 3 {M^+ at *m/z* 382 and fragmentation ions at *m/z* 367 ($M^+ - CH_3$), 340 ($M^+ - CO - CH_2$), 292 [$M^+ - (CH_3)_3SiOH$], 277 [$M^+ - (CH_3)_3Si - OH - CH_3$], 264 [$M^+ - (CH_3)_3SiO - CH - O$], 252 [$M^+ - (CH_3)_3SiO - CH - CO$], 217 [$M^+ - (CH_3)_3SiO - CH - CO - Cl$]}, which has been identified to be 4-(4-chloro-

TABLE 1 Metabolites produced from 4-hydroxy-4′-chlorobiphenyl by B356 BPDO

Metabolite no.[a]	Spectral feature(s) (TMS derivatives)[b]		
	M^+	M-15	Other ions
1	364 (100)	349 (18)	276 (30), 261 (20), 246 (31), 210 (3), 147 (16), 139 (16)
2	382 (13)	367 (20)	339 (6), 264 (40), 249 (14), 217 (169), 204 (100), 147 (63)
3	382 (40)	367 (7)	340 (100), 264 (26), 252 (68), 217 (22), 204 (3), 147 (80)
4	364 (100)	349 (4)	276 (21), 261 (7), 246 (18), 210 (3), 147 (4), 139 (6)
5	452 (100)	437 (5)	364 (5), 349 (60)
6	454 (100)	439 (5)	364 (18), 341 (4), 279 (19), 264 (18),147 (95)
7	452 (100)	437 (5)	417 (1), 379 (2), 364 (7), 349 (28), 321 (8), 314 (1)

[a] Metabolite numbering follows the order of elution on the GC-MS spectrum. The structures are shown in Fig. 2.
[b] Numbers refer to *m/z* values (percentage of the base peak).

TABLE 2 NMR features of metabolite 7

Position no.	Chemical shift[a] (ppm)			
	^1H	^{13}C		
		Experimental[b]	Theoretical molecule A	Theoretical molecule B
1		133.99	136.5	132.5
2	6.716 (s)	106.88	107.0	129.5
3		147.16	143.5	115.0
4		NA	126.5	153.5
5		147.16	143.5	115.0
6	6.716 (s)	106.88	107.0	129.5
1′		141.12	139.5	143.5
2′	7.557 (d)	129.50	129.0	106.5
3′	7.428 (d)	128.98	128.5	157.0
4′		132.88	133.0	106.0
5′	7.428 (d)	128.98	128.5	157.0
6′	7.557 (d)	129.50	129.0	106.5

[a] Theoretical molecule A, 3,4,5-trihydroxy-4′-chlorobiphenyl; theoretical molecule B, 3′,4,5′-trihydroxy-4′-chlorobiphenyl.
[b] NA, not available.

phenyl)-*cis*-5,6-dihydroxycyclohex-3-en-1-one by NMR spectrometry (see below). The TMS-treated metabolite 4 exhibited mass spectral features that, on the basis of previous reports (8, 34), were characteristic of a dihydroxychlorobiphenyl (Table 1). The identity of this metabolite was confirmed by NMR spectroscopy (see below). The spectral features of metabolite 5 corresponded to those of a trihydroxychlorobiphenyl (Table 1), and the spectral features metabolite 6 corresponded to those of a dihydrotrihydroxychlorobiphenyl (Table 1).

Analysis of the metabolites produced from 4-hydroxy-4′-chlorobiphenyl by biphenyl-induced resting cells of strain B356. When a resting suspension of biphenyl-induced B356 cells was incubated with 1.6 μmol/ml of 4-hydroxy-4′-chlorobiphenyl, about 10% of the added substrate remained after 2 h of incubation. In the acidic extract, we detected only approximately 10 nmol/ml of each of 4-chlorobenzoic acid and 4-hydroxybenzoic acid, and both were identified by comparing their spectral features with those of authentic standards. In addition, we detected only traces of a metabolite whose spectral features were identical to those of 2-hydroxy-6-oxo-6-(4′-chlorophenyl)-hexa-2,4-dienoic acid (chlorophenyl-HODA), which is also produced from 2,3-dihydroxy-4′-chlorobiphenyl during the metabolism of 4-chlorobiphenyl (34). Two major metabolites, metabolites 4 and 7, were detected in the neutral extract from cell suspensions incubated for 2 h (Fig. 2). Together, they represented more than 95% of the total neutral plus acidic metabolites, and their GC-MS features were identical to those of metabolites 4 and 7. Since both 4-hydroxybenzoate and 4-chlorobenzoate are poor growth substrates for strain B356 and poorly metabolized by biphenyl-induced cells of strain B356 (not shown), most of the added 1.6 μmol/ml substrate should have been converted to the benzoic acid derivatives by the resting cell suspension after 2 h of incubation. Since less than 1% of the added substrate was converted to the acidic metabolites chlorophenyl-HODA plus hydroxy- and chlorobenzoic acids and since almost 90% of the substrate was converted to metabolite 4 plus metabolite 7, it suggested that the last two compounds were dead-end metabolites that accumulated in the growth medium.

Identities of metabolites 3, 4, and 7. Metabolite 7 was purified as a single peak by HPLC and analyzed by NMR spectrometry. Metabolite 3 was also purified by HPLC, but the purified preparation contained a small amount of metabolite 4. This mixture was also analyzed by NMR spectrometry.

On the basis of its NMR features reported in Table 2, compound 7 was identified to be 3,4,5-trihydroxy-4′-chlorobiphenyl. The presence of only three signals (one singlet and two doublets) for 6 protons shows that the metabolite is perfectly symmetrical; thus, two hydroxyl groups are located on two symmetrical positions of one of the aromatic rings. A two-dimensional (2D) heteronuclear multiple bond correlation (HMBC) experiment showed a correlation between the singlet proton at 6.716 ppm and carbon C-1′ at 141.12 ppm (Fig. 3A), which gives only two possible positions for these hydroxyl groups at either 3,5 or 3′,5′. Therefore, the identity of metabolite 7 was confirmed to be 3,4,5-trihydroxy-4′-chlorobiphenyl on the basis of the experimental chemical shift values for the ^{13}C NMR, which were very close to the calculated theoretical values for this compound (Table 2).

Metabolite 4 was also identified from its NMR spectral features. This metabolite was detected as a minor component of the HPLC peak containing metabolite 3, but the resolution and peak height for the ^1H NMR and the 2D correlation spectroscopy spectra were good enough to allow its identification. The ^1H NMR spectrum showed five signals representing seven protons [peaks at 7.60 ppm (d,2H) (H-2′,H-6′ or H-3′,H-5′) and 7.38 ppm (d,2H) (H-3′,H-5′ or H-2′,H-6′), at 7.15 ppm (d,1H) (H-2), at 7.03 ppm (dd,1H) (H-6), and at 6.94 ppm (d,1H) (H-5)]. The structure and coupling constants shown in Fig. 3B are identical to those already reported for 3,4-dihydroxy-4′-chlorobiphenyl in the same solvent (35). The accumulation of metabolites 4 and 7 in biphenyl-induced cell suspensions of strain B356 may be explained by the inability of B356 BphC to metabolize *meta-para*-dihydroxybiphenyls during the incubation period (36).

The ^1H NMR spectrum of metabolite 3 showed 9 protons, including two couples of symmetrical vicinal aromatic protons (AA′BB′ system) [7.424 ppm (d), 8.5 Hz (2H), and 7.658 ppm (d), 8.5 Hz (2H)]. The correlation between these four protons and the carbon at position 4′ observed from a 2D HMBC spectrum, as well

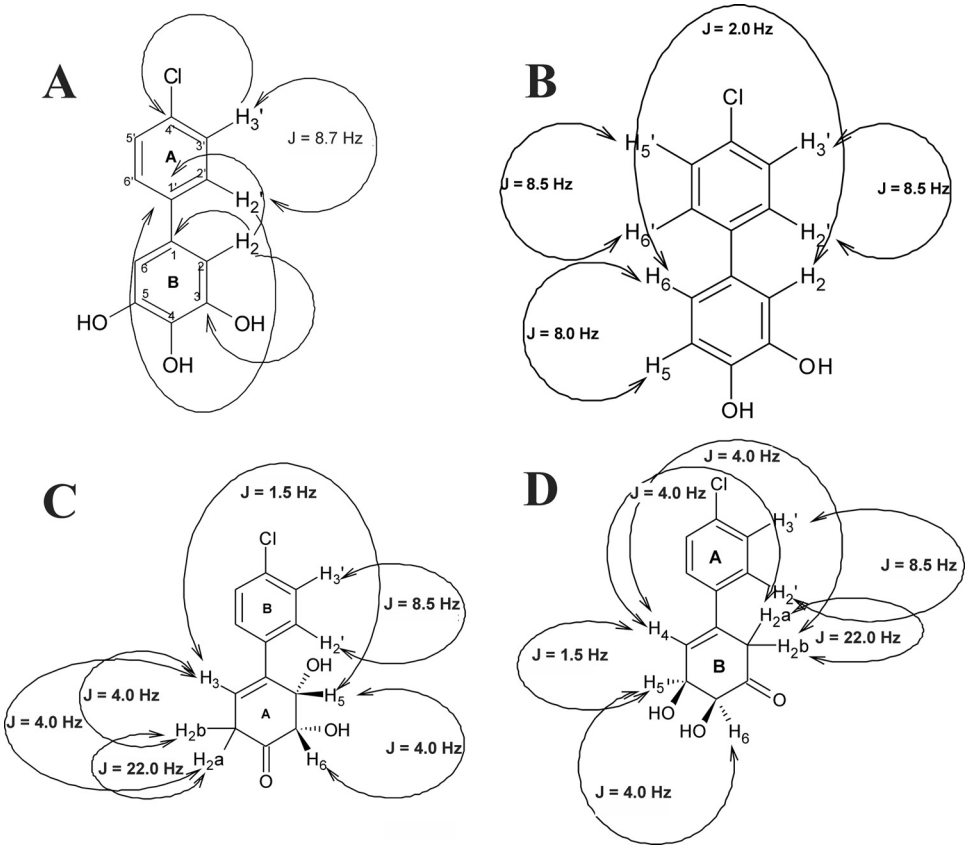

FIG 3 NMR coupling constants and HMBC correlations of 3,4,5-trihydroxy-4′-chlorobiphenyl (metabolite 7) (A) and NMR coupling constants of 3,4-dihydroxy-4′-chlorobiphenyl (metabolite 4) (B), 4-(4-chlorophenyl)-*cis*-5,6-dihydroxycyclohex-3-en-1-one] (molecule 3A) (C), and 3-(4-chlorophenyl)-*cis*-5,6-dihydroxycyclohex-3-en-1-one (molecule 3B) (D).

as the ^{13}C chemical shifts (Table 3), confirmed that one of the two phenyl rings was not transformed during the enzymatic reaction.

Signals for the other ring were one carbonyl (C═O; 207.813 ppm), one methylene (CH_2; C, 39.749 ppm; Ha, 3.365 ppm; Hb, 3.123 ppm), two CH—OH groups (C, 77.605 ppm and 73.706 ppm, respectively; H, 4.892 ppm and 4.649 ppm, respectively), and one CH═ (C, 125.868 ppm; H, 6.371 ppm). On the basis of the HMBC correlations, there were two possible structures of metabolite 3. These possibilities were molecule 3A [4-(4-chlorophenyl)-*cis*-5,6-dihydroxycyclohex-3-en-1-one] (Fig. 3C) or molecule 3B [3-(4-chlorophenyl)-*cis*-5,6-dihydroxycyclohex-3-en-1-one] (Fig. 3D). In the case of molecule 3B (Fig. 3D), there are several unjustifiable coupling constants, such as $J_{H\text{-}4,H\text{-}5}$ equal to 1.5 Hz and $J_{H\text{-}2a,H\text{-}4}$ and $J_{H\text{-}2b,H\text{-}4}$ equal to 4.0 Hz. In addition, for this compound, no four-bond total correlation spectroscopy (TOCSY) correlation was observed between protons H-4, H-5, and H-6.

TABLE 3 ^{13}C and ^{1}H chemical shifts and HMBC correlations of metabolite 3

Position no.	Chemical shift(s) (ppm)		HMBC correlation
	^{13}C	^{1}H	
1	207.813		
2	39.749	2a, 3.365 (dd); 2b, 3.123 (dd)	H-2, C-1, C-3, C-4, C-6, C-5, C-1′, C-2′
3	125.868	6.371 (dt)	H-3, C-4, C-1′, C-5, C-2, C-1
4	138.203		
5	77.605	4.892 (d)	H-5, C-6, C-3, C-4, C-1′, C-1
6	73.706	4.649 (d)	H-6, C-5, C-1
1′	139.837		
2′	128.372	7.658 (d)	H-2′, C-3′, C-4′, C-1
3′	129.423	7.424 (d)	H-3′, C-2′, C-4′, C-1′
4′	133.610		
5′	129.423	7.424 (d)	H-5′, C-2′, C-4′, C-1′
6′	128.372	7.658 (d)	H-6′, C-3′, C4-′, C-1

On the other hand, all coupling constant values were consistent with those for the structure of molecule 3A and also consistent with the results of the TOCSY experiment, which did not show any of the three vicinal protons. The $J_{H\text{-}5,H\text{-}6}$ coupling value at 4.0 Hz reveals a 45-degree dihedral angle (calculated by Karplus equations [37]), consistent with a *cis* conformation. With these pieces of evidence, metabolite 3 was identified to be molecule 3A, which is 4-(4-chlorophenyl)-*cis*-5,6-dihydroxycyclohex-3-en-1-one. The ^{13}C and ^{1}H chemical shifts and HMBC correlations for molecule 3A are listed in Table 3. Both metabolite 2 and metabolite 3 are tautomers of *cis*-2,3-dihydro-2,3,4-trihydroxy-4′-chlorobiphenyl, and the absence of the latter in the medium suggests that the equilibrium is in favor of tautomer formation.

Experimental evidence showing that metabolite 7 is produced from oxidation of metabolite 4. We performed additional experiments to determine whether metabolites 4 and 7 were pro-

duced simultaneously or sequentially. In one set of experiments, we incubated a suspension of IPTG-induced recombinant *E. coli* cells expressing B356 BPDO with 0.8 mM 4-hydroxy-4′-chlorobiphenyl. After a 30-min incubation, approximately 30% of the substrate was metabolized, and on the basis of the GC-MS peak area, metabolites 4 and 7 represented, respectively, 90% and 10% of the total metabolites. Other metabolites, metabolites 1, 2, 3, 5, and 6, were also detected, but in trace amounts. Consistent with a further oxidation of metabolite 4, when the same suspension was incubated for 2 h, more than 90% of the substrate was metabolized, and metabolite 7 was by far the major metabolite, representing 95% of the total metabolites, with small amounts of all other metabolites being detected (not shown). When the suspensions were incubated for 18 h, these minor metabolites disappeared, most likely due to polymerization through oxidation, and metabolite 7 was the only metabolite detected in the culture medium. As indicated above, unlike the experiment performed with recombinant *E. coli* cells expressing B356 BPDO, purified preparations of B356 BPDO generated a pattern of metabolites that remained similar for incubation times of between 2 and 15 min. This may be explained by the fact that 4-hydroxy-4′-chlorobiphenyl was added in excess in the *in vitro* reaction mixtures. It was therefore always present in the medium to compete as the substrate with metabolite 4.

As further evidence that metabolite 7 is produced from metabolite 4, the mixture of metabolites 3 and 4 that was used for NMR analysis was used as the substrate for a purified preparation of B356 BPDO. After a 10-min reaction, metabolite 3 was not metabolized, as shown by the fact that its peak area remained the same, but approximately 85% of metabolite 4 was converted to metabolite 7 (not shown). This shows clearly that metabolite 7 is produced from further oxidation of metabolite 4 by B356 BPDO. It also shows that, once produced, metabolite 3 is a stable tautomer of *cis*-2,3-dihydro-2,3,4-trihydroxy-4′-chlorobiphenyl and is not further transformed by B356 BPDO. In addition, approximately 5% of metabolite 4 was converted to a metabolite whose GC retention time and mass spectral features were identical to those of metabolite 5. This shows that metabolite 5 was also generated from further oxidation of metabolite 4. This metabolite could be the 3,4,6-trihydroxy-4′-chlorobiphenyl produced from 5,6-dihydro-3,4,5,6-tetrahydroxy-4′chlorobiphenyl after the removal of one water molecule at position 5. However, it could also be the 2,3,4-trihydroxy-4′-chlorobiphenyl which may result from the dioxygenation of 3,4-dihydroxy-4′-chlorobiphenyl on carbons 2 and 4.

Interestingly, under the same conditions, *E. coli* cells producing LB400 BPDO metabolized less than 10% of the added 4-hydroxy-4′-chlorobiphenyl in 18 h and 3,4-dihydroxy-4′-chlorobiphenyl was the sole metabolite detected in those suspensions. Since this experiment included controls that showed that the same cell suspension metabolized 4-chlorobiphenyl as efficiently as *E. coli* cells expressing B356 BPDO, we may conclude that, unlike B356 BPDO, LB400 BPDO metabolized 4-hydroxy-4′-chlorobiphenyl poorly and it was unable to further metabolize the reaction product.

Docking experiments and suggested pathways for metabolism of 4-hydroxy-4′-chlorobiphenyl. We docked 4-hydroxy-4′-chlorobiphenyl in the substrate-bound form of $BphAE_{B356}$ after removal of biphenyl. The conformation of 19 of the 20 top-ranked docked molecules in $BphAE_{B356}$ exhibited an orientation very similar to the one shown in Fig. 4A. The *ortho-meta* carbons did not closely align with carbons 2 and 3 of the oxidized ring of biphenyl in the complexed form (Fig. 4A), but they were at a distance from the catalytic iron that would allow an oxygenation of the molecule onto those positions. For all of them, the *ortho-meta* carbons were not perfectly equidistant to the catalytic iron but were at a distance of between 3.7 and 4.0 Å, which is in the range of the distance between the reactive atoms of biphenyl and the catalytic iron that was observed (Fig. 4A). A similar observation was made in a previous work (38) with 1,1,1-trichloro-2,2-bis(4-chlorophenyl)ethane (DDT), a doubly *para*-substituted biphenyl analog, where the *ortho-meta* carbons of DDT did not closely align with those of the oxidized ring of biphenyl in the complexed form. It is likely that if the docking process had aligned the *ortho-meta* carbons of these substrates closer to those of biphenyl, the *para* substituent would have been too close to Gln226 and Phe227, two residues that are involved in the catalytic reaction (31). Therefore, these analogs require induced-fit conformational changes of the protein that our docking experiments could not reproduce.

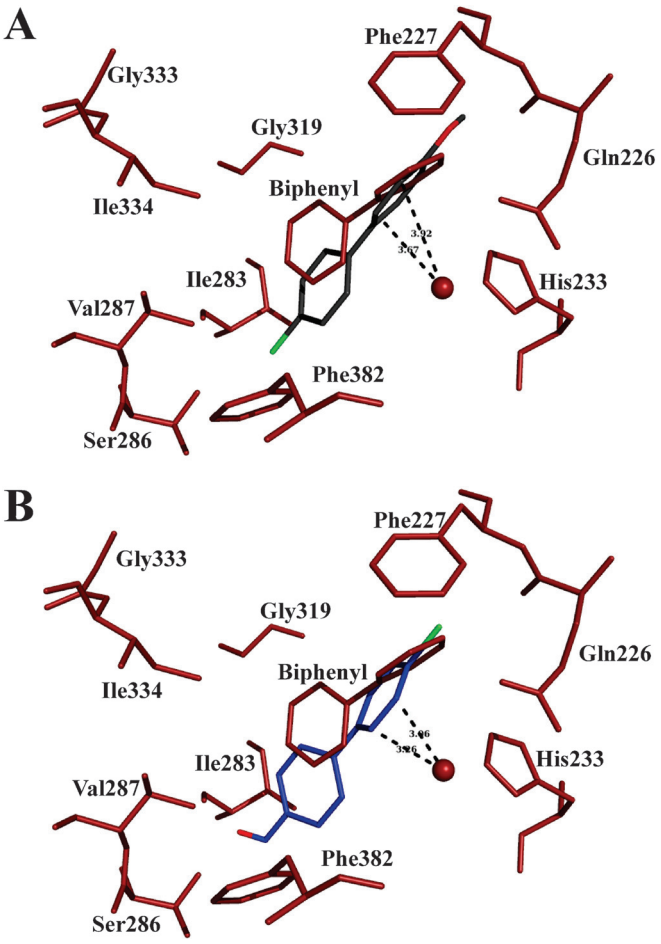

FIG 4 Superposition of catalytic center residues of 4-hydroxy-4′-chlorobiphenyl-docked (black and blue) and biphenyl-bound (red) forms of $BphAE_{B356}$. (A) Major conformation of the docked 4-hydroxy-4′-chlorobiphenyl; (B) minor conformation of the docked 4-hydroxy-4′-chlorobiphenyl. The hydroxyl groups of 4-hydroxy-4′-chlorobiphenyl are in red, and the chlorine atoms are in green. The red spheres represent the catalytic iron.

Among the 20 top-ranked docked molecules, only one exhibited a conformation that would enable an oxygenation of the *ortho-meta* carbons of the chlorinated ring (Fig. 4B). In this case, however, its *ortho-meta* carbons were more distant than those of the other top-ranked molecules to the corresponding carbons of the biphenyl substrate, and in addition, they were at a shorter distance (almost 1 Å less) from the catalytic iron than the *ortho-meta* carbons of the bound biphenyl substrate. This may explain why metabolite 6, which may be the 2′,3′-dihydro-2′,3′,4-trihydroxy-4′-chlorobiphenyl, was a minor product.

On the other hand, although based on model structures only, none of the docking experiments placed 4-hydroxy-4′-chlorobiphenyl in an orientation that would allow a *meta-para* reaction. Therefore, on the basis of the docking experiments, it appears unlikely that 3,4-dihydroxy-4′-chlorobiphenyl was produced from a 3,4-dioxygenation of 4-hydroxy-4′-chlorobiphenyl. It was, rather, metabolized through an *ortho-meta* oxygenation to generate *cis*-2,3-dihydro-2,3,4-trihydroxy-4′-chlorobiphenyl, which appears to be very susceptible to rearrangement.

When purified preparations of B356 BPDO were used to catalyze the oxidation of 4-hydroxy-4′-chlorobiphenyl, about 30% of 2,3-dihydro-2,3,4-trihydroxy-4′-chlorobiphenyl tautomerizes to metabolites 2 and 3. These two tautomers were produced in much larger proportions when the reactions were catalyzed by purified B356 BPDO preparations than when they were catalyzed by biphenyl-induced B356 cells or recombinant *E. coli* cell suspensions producing B356 BPDO. This difference may be explained by the fact that *in vitro* BPDO reactions were performed under conditions (50 mM MES, pH 6.0) that differed significantly from those inside the cells. Although our experimental setting did not allow us to determine the precise conditions that favor tautomerization of 2,3-dihydro-2,3,4-trihydroxy-4′-chlorobiphenyl, once produced, the tautomers were stable in a way similar to that for 3,4-dihydroxy-5-(3-hydroxyphenyl)-5-cyclohexen-1-one, which was produced from *cis*-5,6-dihydro-3,3′,5,6-tetrahydroxybiphenyl during catalytic oxygenation of 3,3′-dihydroxybiphenyl by B356 BPDO (39).

On the other hand, on the basis of biochemical and docking experiments, the preferred pathway for the oxidation of 4-hydroxy-4′-chlorobiphenyl by B356 BPDO would be through the rapid transformation of *cis*-2,3-dihydro-2,3,4-trihydroxy-4′-chlorobiphenyl to 3,4-dihydroxy-4′-chlorobiphenyl (metabolite 4) through water removal at position 2, followed by a further oxidation of this metabolite to ultimately generate metabolite 7 and a small amount of metabolite 5. We tried to dock 3,4-dihydroxy-4′-chlorobiphenyl into $BphAE_{B356}$, but none of the 20 top-ranked molecules exhibited a productive conformation (not shown); other structural features that our docking experiments could not reproduce are required for productive binding of this substrate. Therefore, we are unable to determine precisely whether the oxygenation reaction of metabolite 4 occurred onto carbons 5,6 or carbons 4,5. However, on the basis of the docking experiments with 4-hydroxy-4′-chlorobiphenyl, which favored the *ortho-meta* dioxygenation of the substrate, and also on the basis of the finding that oxidation of metabolite 4 yielded a small amount of metabolite 5, we may postulate that metabolite 4 was oxygenated onto carbons 5,6 and the resulting dihydrodihydroxy metabolite was dehydrated principally at position 6 to generate metabolite 7.

A small portion of the 2,3-dihydro-2,3,4-trihydroxy-4′-chlorobiphenyl produced from the BPDO reaction may lose one water molecule at position 4 to generate 2,3-dihydroxy-4′-chlorobiphenyl (metabolite 1), but this pathway is minor, since only a small amount was detected in the medium.

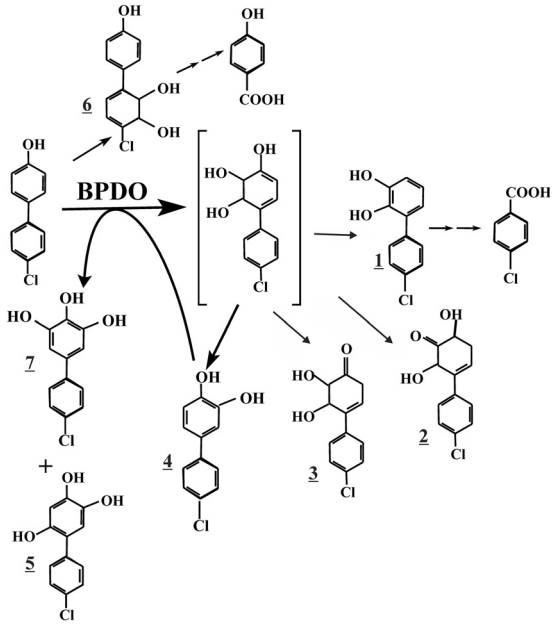

FIG 5 Proposed profile of metabolites produced from 4-hydroxy-4′-chlorobiphenyl by B356 BPDO and biphenyl-induced cells of strain B356. Thick arrows, the major routes of transformation; brackets, the metabolite was not detected. The metabolite numbering is as indicated in Table 1.

Because 4-hydroxybenzoate was found among the metabolites in the acid extract of B356 resting cell suspensions, we may presume that metabolite 6 was 2′,3′-dihydro-2′,3′,4-trihydroxy-4′-chlorobiphenyl. This would be consistent with the findings of the docking experiments that showed that 1 of 20 docked molecules exhibited a conformation allowing an oxygenation of the chlorinated ring. However, we cannot exclude the possibility that metabolite 6 would be the 2,3-dihydro-2,3,4-trihydroxy-4′-chlorobiphenyl that tautomerizes to metabolites 2 and 3.

On the basis of these observations, we may propose the metabolic pathway for 4-hydroxy-4′-chlorobiphenyl shown in Fig. 5.

Metabolism of other *para*-hydroxy- or hydroxychlorobiphenyls. Analysis of the metabolites generated from 4-hydroxy-4′-chlorobiphenyl showed that oxidation of this doubly *para*-substituted biphenyl by the biphenyl dioxygenase may proceed through various pathways that involve the rearrangement of *cis*-2,3-dihydro-2,3,4-trihydroxy-4′-chlorobiphenyl. In order to verify that this observation was not a feature unique to this substrate, we also examined the metabolism of 4,4′-dihydroxybiphenyl, 3-hydroxy-4,4′-dichlorobiphenyl, and 3,3′-dihydroxy-4,4′-dichlorobiphenyl.

Metabolism of 4,4′-dihydroxybiphenyl by biphenyl-induced cells of strain B356. When a biphenyl-induced resting cell suspension of strain B356 was incubated with 4,4′-dihydroxybiphenyl, several metabolites were detected. We did not investigate in detail the metabolites that were produced, and our data do not allow us to draw a precise profile of the metabolites. However, in the acid fraction, we detected a small amount of 4-hydroxybenzoic acid (not shown), showing that part of the substrate was metabolized to the end product of the pathway. When the reaction was catalyzed by *E. coli* cells expressing B356 BPDO, more than 95% of the substrate was converted to a metab-

TABLE 4 Metabolites produced from 4,4′-dihydroxybiphenyl by strain B356 BPDO

Metabolite structure	Metabolite no.[a]	Spectral feature(s) (no. of TMS derivatives)[b]		
		M^+	M-15	Other ions
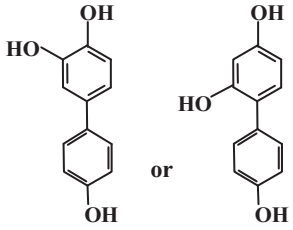	**8**	418 (52)	403 (3)	330 (7), 315 (10), 299 (3), 241 (3), 209 (2), 147 (4), 73 (100)
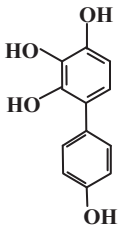	**9**	506 (100)	491 (1)	418 (13), 403 (8), 300 (1), 253 (1), 207 (12), 147 (10), 73 (95)
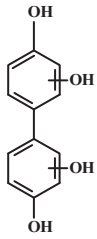	**10**	506 (50)	491 (3)	418 (5), 403 (1), 300 (1), 253 (1), 207 (1), 147 (5), 73 (100)
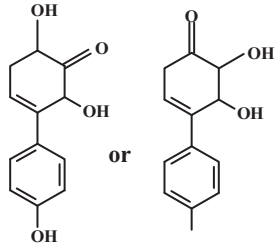	**11**	436 (1)	421 (13)	330 (40), 204 (100)

[a] Metabolite numbering follows the order of elution on the GC-MS spectrum.
[b] Numbers refer to *m/z* values (percentage of the base peak).

olite exhibiting the spectral features of a trihydroxybiphenyl (metabolite 8; Table 4). The fact that this metabolite was not further metabolized by BphC (not shown) allows us to tentatively identify it as 3,4,4′-trihydroxybiphenyl, which BphC would be unable to cleave (36), or as 2,4,4′-trihydroxybiphenyl. No dihydrodihydroxy metabolites were detected, but two tetrahydroxybiphenyls (metabolites 9 and 10; Table 4) were produced in small amounts. Together, they represented less than 1% of the total metabolites. We also detected trace amounts of a metabolite which, on the basis of its mass spectral features, was tentatively identified as 5,6-dihydroxy-4-(4-hydroxyphenyl)-cyclohex-3-en-1-one or 2,6-dihydroxy-4-(4-hydroxyphenyl)-cyclohex-3-en-1-one. Obviously, analogs with different distributions of their hydroxyl and ketone functions (metabolite 11; Table 4), which would be tautomers of 2,3-dihydro-2,3,4,4′-tetrahydroxybiphenyl resulting from the dioxygenation of the substrate on carbons 2 and 3, could be considered. Together, these observations plus the absence of 2,3-dihydro-2,3,4,4′-tetrahydroxybiphenyl in recombinant *E. coli* cell suspensions provide evidence that this metabolite is susceptible to rearrangement during the oxygenase reaction. Metabolite 8 would most likely be produced from 2,3-dihydro-2,3,4,4′-tetrahydroxybiphenyl after the spontaneous removal of water. When *E. coli* cells expressing LB400 BPDO were used to metabolize 4,4′-dihydroxybiphenyl, as was the case for 4-hydroxy-4′-

TABLE 5 Metabolites produced from 3-hydroxy-4,4′-dichlorobiphenyl and from 3,3′-dihydroxy-4,4′-dichlorobiphenyl by strain B356 and its BPDO

Metabolite no.[a]	Spectral feature(s) (no. of TMS derivatives)[b]		
	M^+	M-15	Other ions
12	316 (21)	301 (100)	257 (35), 227 (18), 189 (10), 149 (7)
13	398 (100)	383 (11)	363 (3), 348 (32), 333 (9), 275 (7), 239 (10), 181(3), 152 (3), 131 (7)
14	452 (100)	437 (7)	417 (1), 379 (2), 364 (2), 349 (93), 314 (26), 299 (1), 253 (7), 147 (6)
15	416 (1)	401 (2)	353 (6), 266 (100), 250 (1), 147 (27)
16	486 (100)	471 (6)	398 (7), 383 (68), 348 (50), 219 (13), 147 (6), 131 (14)
17	470 (3)	455 (9)	381 (5), 354 (100), 315 (4), 271 (6), 181 (8), 147 (19), 131 (91)

[a] Metabolite numbering follows the order of elution on the GC-MS spectrum. Structures are shown in Fig. 6 and 7.
[b] Numbers refer to *m/z* values (percentage of the base peak).

chlorobiphenyl, the substrate was poorly utilized. Less than 5% of the substrate was converted to metabolite 8, which was the only one recovered in the culture medium. Therefore, LB400 BPDO catalyzed the oxidation of 4,4′-dihydroxybiphenyl less efficiently than B356 BPDO did, but both of them produced the same major metabolite, and they did not produce the expected dihydrodihydroxy metabolites.

Metabolism of 3-hydroxy-4,4′-dichlorobiphenyl. When 3-hydroxy-4,4′-dichlorobiphenyl was used as the substrate for biphenyl-induced resting cell suspensions of strain B356, less than 20% of the added substrate was metabolized. The major metabolite, representing approximately 50% of the total (neutral plus acidic) metabolites, was 3-hydroxy-4-chlorobenzoic acid (metabolite 12; Table 5), which was identified on the basis of its GC-MS spectral features. Among the several hydroxylated metabolites detected, only two were produced in significant amounts, and each of these represented about 25% of the total metabolites. The first was identified as a dihydroxydichlorobiphenyl on the basis of its mass spectral features (metabolite 13; Table 5). It may result from 2,3-dihydro-2,3,3′-trihydroxy-4,4′-dichlorobiphenyl or 5′,6′-dihydro-3′,5′,6′-trihydroxy-4,4′-dichlorobiphenyl after elimination of one water molecule. The other was identified as a monochlorotrihydroxybiphenyl on the basis of its mass spectral features (metabolite 14; Table 5). When purified B356 BPDO was used to metabolize 3-hydroxy-4,4′-dichlorobiphenyl, less than 5% of the substrate was transformed within 10 min and metabolite 13 was a minor product, on the basis of the area under its GC-MS peak, representing less than 5% of the total metabolites. Two major products were detected at approximately equal amounts and together constituted about 90% of the total metabolites. The mass spectral features of the first one to elute (spectrum not shown) were identical to those of metabolite 14 produced by biphenyl-induced resting cells of strain B356. This could be produced by hydroxylation of the nonhydroxylated ring with concomitant dechlorination of the ring, resulting in 2,3,3′-trihydroxy-4′-chlorobiphenyl. Production of metabolite 14 would be consistent with the observation that 3-hydroxy-4-chlorobenzoic acid is a major metabolite of B356 resting cell suspensions. The second major metabolite was identified on the basis of its mass spectral features to be either 6-chloro-3-(4-chlorophenyl)-4,5-dihydroxycyclohex-2-en-1-one or 6-chloro-3-(4-chlorophenyl)-2,5-dihydroxycyclohex-3-en-1-one (metabolite 15; Table 5). It exhibited a molecular ion at *m/z* 416 and fragmentation ions at *m/z* 401 (M^+-CH_3) and at *m/z* 381 (M^+-Cl), with a single prominent ion at *m/z* 266 corresponding to (M^+-150), which would result from the loss of [$(CH_3)_3$SiOH-CH-CH-Cl]. This is similar to the prominent *m/z* M^+-116 ions corresponding to [$(CH_3)_3$SiOH-CH-CH_2] observed for 3,4-dihydroxy-5-(3-hydroxyphenyl)-5-cyclohexen-1-one (8), which is characterized by the fact that the two *meta* positions of the nonaromatic ring are occupied by a hydroxyl and a carbonyl group, respectively, and one of the *ortho* positions is occupied by a hydroxyl group. Altogether, the data presented above show that both rings of 3-hydroxy-4,4′-dichlorobiphenyl may be attacked by B356 BPDO. When the nonhydroxylated ring is oxidized, the resulting metabolite may easily lose the *para* chlorine atom to generate a catechol which is further metabolized by the downstream enzymes. However, our data did not allow us to determine the mechanism involved in the reductive dehalogenation of the biphenyl ring during catalytic oxygenation. When the hydroxylated ring is oxygenated by B356 BPDO, the resulting metabolite is readily tautomerized, since no 5′,6′-dihydro-3′,5′,6′-trihydroxy-4,4′-chlorobiphenyl was detected in the reaction medium. Since neither the latter nor its tautomer (metabolite 15) was detected in biphenyl-induced resting cell suspensions of strain B356 and 4-chlorobenzoic acid was absent, the suggestion is that the dihydrodihydroxy metabolite may be further oxidized or polymerized to a nondetectable dead-end product in the cell suspensions. A tentative pathway for the metabolism of 4,4′-dichloro-3-hydroxybiphenyl is proposed in Fig. 6.

Metabolism of 3,3′-dihydroxy-4,4′-dichlorobiphenyl. 3,3′-Dihydroxy-4,4′-dichlorobiphenyl is poorly metabolized by strain B356. About 1% of the substrate added to the biphenyl-induced resting cell suspension was metabolized after 18 h of incubation. The major metabolite, representing about 90% of the total, was detected in the acidic extract of the culture, and it was identified as

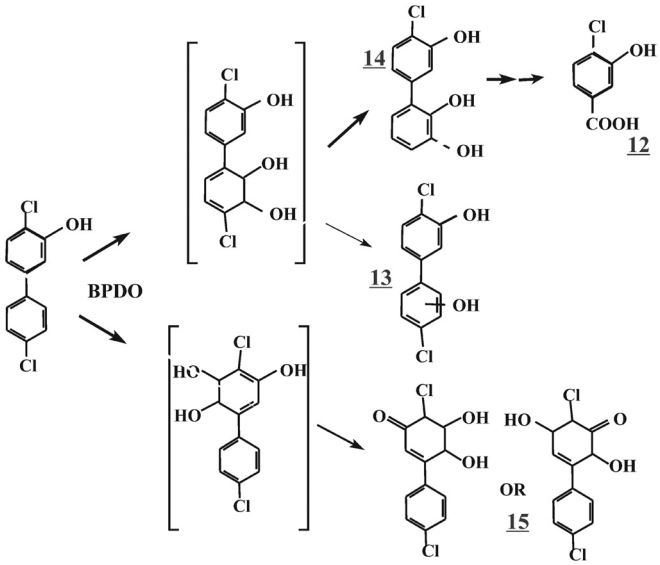

FIG 6 Tentative profile of metabolites produced from 3-hydroxy-4,4′-dichlorobiphenyl by B356 BPDO and biphenyl-induced cells of strain B356. Thick arrows, the major routes of transformation; brackets, the metabolite was not detected. The metabolite numbering is as indicated in Table 5.

3-hydroxy-4-chlorobenzoic acid on the basis of its GC-MS spectral features, which were identical to those of metabolite 12 (Table 5). The other metabolites were hydroxychlorobiphenyls, which were found at very low concentrations and were not further identified. The observation that the biphenyl catabolic enzymes of strain B356 poorly metabolized 3,3′-dihydroxy-4,4′-dichlorobiphenyl was confirmed by the fact that less than 1% of the added substrate was metabolized after 10 min of incubation with a purified preparation of B356 BPDO. Only one major metabolite was detected, and it exhibited the mass spectral attributes of a trihydroxydichlorobiphenyl (metabolite 16; Table 5). Although further work will be required to determine its precise identity, this metabolite may presumably be the 2,3,3′-trihydroxy-4,4′-dichlorobiphenyl that would be further metabolized by the downstream biphenyl catabolic enzymes to generate the 3-hydroxy-4-chlorobenzoic acid found in the resting cell suspensions of strain B356. Metabolite 16 was most likely produced from a 2,3 dioxygenation reaction with concomitant replacement of the *meta* hydroxyl, but we cannot exclude the possibility that it was formed from a 5,6 dioxygenation followed by elimination of one water molecule. Another metabolite detected in a trace amount in the BPDO reaction medium was identified on the basis of its mass spectral features, which were characteristic of those of a monochlorinated compound, as either 3-(4-chloro-3-hydroxyphenyl)-2,5-dihydroxycyclohex-3-en-1-one or 3-(4-chloro-3-hydroxyphenyl)-4,5-dihydroxycyclohex-2-en-1-one (metabolite 17; Table 5). The metabolite exhibited the characteristic single prominent ion at *m/z* 354 (M^+-116), corresponding to the $(CH_3)_3SiOH\text{-}CH\text{-}CH_2$ observed for 3,4-dihydroxy-5-(3-hydroxyphenyl)-5-cyclohexen-1-one (8). This metabolite is not likely to be further metabolized by the biphenyl catabolic pathway and is most likely produced from the concomitant tautomerization and loss of a chlorine atom of 5,6-dihydro-3,3′,5,6-tetrahydroxy-4,4′-dichlorobiphenyl that would result from a catalytic oxygenation on carbons 5 and 6. It is noteworthy that in the case of 3-hydroxy-4,4′-dichlorobiphenyl, the attack onto the hydroxylated ring generated a similar metabolite (metabolite 15), but it was not dehalogenated. This finding suggests that the occurrence of the dehalogenation reaction may depend on the overall electronic distribution of the dihydrodihydroxy metabolite. A tentative pathway for the metabolism of 4,4′-dichloro-3,3′-dihydroxybiphenyl is presented in Fig. 7.

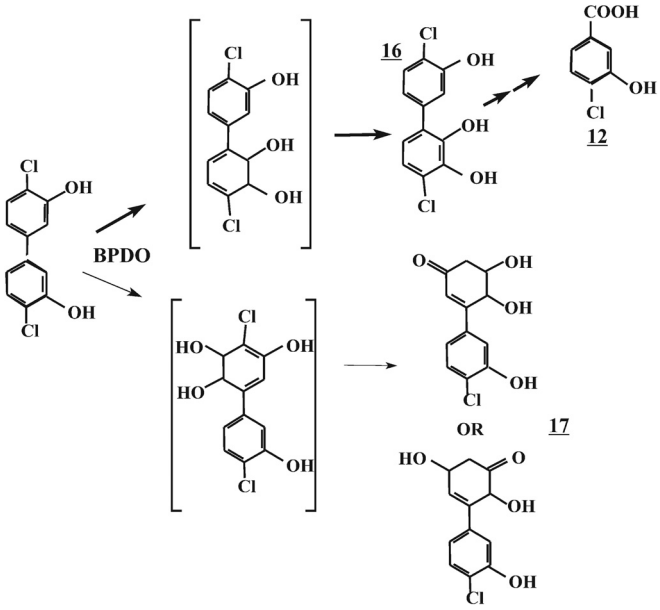

FIG 7 Tentative profile of metabolites produced from 3,3′-dihydroxy-4,4′-dichlorobiphenyl by B356 BPDO and biphenyl-induced cells of strain B356. Thick arrows, the major routes of transformation; brackets, the metabolite was not detected. The metabolite numbering is as indicated in Table 5.

DISCUSSION

According to their primary amino acid sequences, $BphAE_{B356}$ and $BphAE_{LB400}$ belong to distinct phylogenetic clusters of BphAEs. Recent data have suggested that each cluster may have evolved to play distinct ecophysiological roles with respect to the metabolism of aromatic compounds in the environment (13, 20). Although LB400 BPDO has been considered the best PCB-metabolizing dioxygenase of natural origin, B356 BPDO was shown to metabolize many biphenyl analogs more efficiently than LB400 BPDO (13, 19, 20, 38). Consistent with these findings, in this work we showed that strain B356 BPDO metabolizes several *para*-substituted hydroxy- and hydroxychlorobiphenyl analogs more efficiently than strain LB400 BPDO. Our data also showed that the dihydrodihydroxybiphenyls resulting from catalytic dioxygenation of doubly *para*-substituted hydroxychlorobiphenyls are prone to extensive intermolecular rearrangements which may or may not lead to the loss of water or of a *para* chlorine atom. Similar instabilities and rearrangements were observed in the case of 5,6-dihydro-3,3′,5,6-tetrahydroxybiphenyl, which was generated from the catalytic oxygenation of 3,3′-dihydroxybiphenyl by B356 BPDO and which was rapidly rearranged to a stable tautomer [(3*S*,4*R*)-3,4-dihydroxy-5-(3-hydroxyphenyl)-5-cyclohexen-1-one] that was not further metabolized by the biphenyl catabolic enzymes (8, 39).

In a previous work, it was shown that *Pseudomonas putida* DA261 which expressed B356 BPDO plus BphB produced 2,3-dihydroxy-4′-chlorobiphenyl and 2,3-dihydroxy-2′-chlorobiphenyl from 4,4′-dichlorobiphenyl and 2,4-dichlorobiphenyl, respectively (40). This suggested that a dehalogenation reaction had occurred during catalytic oxygenation of the *para*-chlorinated ring by B356 BPDO (40). During this work, we confirmed this observation and found that 2,3-dihydroxy-4′-chlorobiphenyl was a major metabolite produced from 4,4′-dichlorobiphenyl by *E. coli* cells expressing B356 BPDO (not shown). In addition, in this work a similar dehalogenation reaction was observed with other doubly *para*-substituted biphenyls. Thus, we found that 2,3,3′-trihydroxy-4′-chlorobiphenyl (metabolite 14) was a major metabolite produced from 3-hydroxy-4,4′-chlorobiphenyl and a small amount of 3-(4-chloro-3-hydroxyphenyl)-2,5-dihydroxycyclohex-3-en-1-one (metabolite 17) was produced from 3,3′-dihydroxy-4,4′-dichlorobiphenyl by a purified preparation of B356 BPDO. These dehalogenation reactions are distinct from the oxygenolytic dehalogenation occurring during the catalytic oxygenation of the *ortho-meta* carbons of 2,2′-dichlorobiphenyl (41), since the *para* chlorine that was removed was not replaced by an hydroxyl group.

On the other hand, no dechlorinated metabolite was reported when 4,4′-dichlorobiphenyl and 2,4,4′-trichlorobiphenyl were oxidized by *Pseudomonas pseudoalcaligenes* KF707 BPDO (42, 43). Similarly, the catalytic oxidation of 2,4,4′-trichlorobiphenyl and 2,2′,4,4′-tetrachlorobiphenyl by B356 BPDO and by LB400 mutants generated as the major metabolite for each

substrate the expected, nondechlorinated dihydrodihydroxy metabolite, which was stable (19, 44). It is also noteworthy that in a previous work, the *cis*-2,3-dihydro-2,3-dihydroxy-1,1,1-trichloro-2,2-bis(4-chlorophenyl)ethane produced from the catalytic oxygenation of DDT was shown to be very stable and no *para* dehalogenation was observed (38). Furthermore, in the current work no dehalogenated metabolite was detected when 4-hydroxy-4′-chlorobiphenyl was metabolized by B356 BPDO. Therefore, it appears that the dehalogenation reaction occurring during catalytic oxygenation of doubly *para*-substituted chloro- and hydroxychlorobiphenyl analogs may depend on many factors, which may include the number, type, and position of the substituents and perhaps the structural properties of the BPDO used to catalyze the reaction. Further investigation will be required to clarify the mechanism behind this unusual reaction.

On the basis of the findings of the docking experiments, the pathway that we proposed to explain the formation of metabolites 4 and 7 from 4-hydroxy-4′-chlorobiphenyl proceeds through a 2,3 dioxygenation, followed by a redistribution of the electronic configuration of the unstable dihydrodihydroxybiphenyl metabolite. However, other mechanisms may have been involved in their production, and one of these may be substrate displacement during the catalytic reaction. For example, in a previous investigation it was shown that the crystal structure of the dibenzofuran-bound form of a $BphAE_{LB400}$ mutant clearly showed the substrate in the conformation that would enable an angular dioxygenation of dibenzofuran. However, during the catalytic reaction, dibenzofuran (31, 45) was displaced in the catalytic pocket to favor a lateral dioxygenation. Therefore, in the present study, although the docking experiments were consistent with an *ortho-meta* dioxygenation of 4-hydroxy-4′-chlorobiphenyl, we cannot exclude the possibility that the enzyme's regiospecificity toward this substrate may have changed during the catalytic reaction through a similar mechanism to generate principally *meta-para*-hydroxylated metabolites. Likewise, we cannot exclude the possibility that B356 BPDO may have hydroxylated the *meta* carbon of the *para*-hydroxylated ring through a monooxygenase type of reaction similar to the one catalyzed by *P. pseudoalcaligenes* KF707 BPDO on isoflavan-4-ol (46).

Whether metabolite 7 was produced from a 2,3 or a 3,4 oxygenation of the biphenyl molecule, it is noteworthy that this metabolite results from a further oxidation of metabolite 4. In a previous investigation, 3-benzylcyclohexa-3,5-diene-1,2-diol was further oxidized to 3-[(5,6-dihydroxycyclohexa-1,3-dien-1-yl)methyl]cyclohexa-3,5-diene-1,2-diol by B356 BPDO (20). A sequential reaction was also observed when a purified preparation of *Pseudomonas* sp. strain NCBI9816-4 naphthalene dioxygenase was used to catalyze the oxidation of ethylbenzene (47).

Furthermore, when B356 BPDO was coupled to the 2,3-dihydro-2,3-dihydroxybiphenyl dehydrogenase (BphB) of B356, benzophenone was almost completely oxidized to 2,2′,3,3′-tetrahydroxybenzophenone, resulting from the further oxidation of 2,3-dihydroxybenzophenone. Unlike B356 BPDO, LB400 BPDO was unable to further oxidize 3-benzylcyclohexa-3,5-diene-1,2-diol or 2,3-dihydroxybenzophenone (20). This observation, in addition to the fact that metabolite 7 was not detected when 4-hydroxy-4′-chlorobiphenyl was oxidized by LB400 BPDO, provides evidence that BPDOs may further oxidize the initial dihydroxy or dihydrodihydroxy metabolites generated by the catalytic oxygenation of selected biphenyl analogs, but this reaction is structure dependent.

One clear observation made in this work is that B356 and LB400 BPDO reactions produced many metabolites other than the expected 2,3-dihydrodihydroxybiphenyls that would result from an *ortho-meta* dioxygenation of the substrates. A major consequence of this finding is that doubly *para*-substituted hydroxychlorobiphenyls are prone to generate dead-end metabolites when they serve as the substrate for the bacterial biphenyl dioxygenase. This was evidenced by the fact that only small amounts of hydroxy- or chlorobenzoic acids were detected in biphenyl-induced cell suspensions of strain B356 incubated with 4,4′-dihydroxy- or 4-hydroxy-4′-chlorobiphenyl; most of the metabolites were recovered as hydroxylated derivatives of the tested substrates. The formation of dead-end metabolites may also explain why Tehrani et al. (16) did not detect any 4-chlorobenzoate in biphenyl-induced cell suspensions of strain LB400 incubated with 4-hydroxy-4′-chlorobiphenyl, although substrate depletion was observed.

Unlike bacteria which metabolize PCBs using biphenyl dioxygenase to generate *cis*-dihydrodihydroxybiphenyl derivatives, plants and animals principally produce monohydroxylated derivatives from PCBs. In both types of organisms, the hydroxylation may occur on either one of the chlorinated or nonchlorinated rings (6, 48). However, in the case of plants, several reports indicate that the hydroxylation reaction often occurs on the *para* carbon of the least chlorinated ring (6, 22). Altogether, our data show that many hydroxylated metabolites other than those expected for a 2,3 dioxygenation of the substrate are produced when doubly *para*-substituted hydroxychlorobiphenyls are metabolized by the bacterial BPDOs. Some of these, such as the one resulting from *para* dehalogenation reactions, may be metabolized further, but other metabolites may not be further degraded by the biphenyl catabolic enzymes and they may accumulate in the environment. Further work will be required to clarify precisely the mechanisms by which all the metabolites observed in this work were produced. Our data show that a clear picture of the fate of PCBs in contaminated sites will require a better understanding of the metabolism of the hydroxychlorobiphenyls derived from plants, animals, and fungi as well as the chemistry of the dihydrodihydroxylated metabolites produced from them by the bacterial biphenyl dioxygenase.

ACKNOWLEDGMENTS

This work was supported in part by NSERC grant RGPIN/39579-2012 to M. Sylvestre.

We thank Sameer Al-Abdul-Wahid, QANUC NMR Facility (McGill University, Montreal, Quebec, Canada), for his help with NMR analysis.

REFERENCES

1. **Prindle RF.** 1983. Phenolic compounds, p 197–224. *In* Block SS (ed), Disinfection, sterilization and preservation. Lea and Febiger, Philadelphia, PA.
2. **Mohammadi M, Sylvestre M.** 2005. Resolving the profile of metabolites generated during oxidation of dibenzofuran and chlorodibenzofurans by the biphenyl catabolic pathway enzymes. Chem Biol **12:**835–846. http://dx.doi.org/10.1016/j.chembiol.2005.05.017.
3. **Nojiri H, Omori T.** 2002. Molecular bases of aerobic bacterial degradation of dioxins: involvement of angular dioxygenation. Biosci Biotechnol Biochem **66:**2001–2016. http://dx.doi.org/10.1271/bbb.66.2001.
4. **Sylvestre M.** 2013. Prospects for using combined engineered bacterial enzymes and plant systems to rhizoremediate polychlorinated biphenyls. Environ Microbiol **15:**907–915. http://dx.doi.org/10.1111/1462-2920.12007.

5. **Mackova M, Vrchotova B, Francova K, Sylvestre M, Tomaniova M, Lovecka P, Demnerova K, Macek T.** 2007. Biotransformation of PCBs by plants and bacteria—consequences of plant-microbe interactions. Eur J Soil Biol **43:**233–241. http://dx.doi.org/10.1016/j.ejsobi.2007.02.006.
6. **Rezek J, Macek T, Mackova M, Triska J, Ruzickova K.** 2008. Hydroxy-PCBs, methoxy-PCBs and hydroxy-methoxy-PCBs: metabolites of polychlorinated biphenyls formed in vitro by tobacco cells. Environ Sci Technol **42:**5746–5751. http://dx.doi.org/10.1021/es800445h.
7. **Ueno D, Darling C, Alaee M, Campbell L, Pacepavicius G, Teixeira C, Muir D.** 2007. Detection of hydroxylated polychlorinated biphenyls (OH-PCBs) in the abiotic environment: surface water and precipitation from Ontario, Canada. Environ Sci Technol **41:**1841–1848. http://dx.doi.org/10.1021/es061539l.
8. **Sondossi M, Barriault D, Sylvestre M.** 2004. Metabolism of 2,2′- and 3,3′-dihydroxybiphenyl by the biphenyl catabolic pathway of *Comamonas testosteroni* B-356. Appl Environ Microbiol **70:**174–181. http://dx.doi.org/10.1128/AEM.70.1.174-181.2004.
9. **Tehrani R, Van Aken B.** 2013. Hydroxylated polychlorinated biphenyls in the environment: sources, fate, and toxicities. Environ Sci Pollut Res Int **21:**6334–6345. http://dx.doi.org/10.1007/s11356-013-1742-6.
10. **Francova K, Mackova M, Macek T, Sylvestre M.** 2004. Ability of bacterial biphenyl dioxygenases from *Burkholderia* sp. LB400 and *Comamonas testosteroni* B-356 to catalyse oxygenation of *ortho*-hydroxychlorobiphenyls formed from PCBs by plants. Environ Pollut **127:**41–48. http://dx.doi.org/10.1016/S0269-7491(03)00257-4.
11. **Sondossi M, Sylvestre M, Ahmad D, Masse R.** 1991. Metabolism of hydroxybiphenyl and chloro-hydroxybiphenyl by biphenyl/chlorobiphenyl degrading *Pseudomonas testosteroni* strain B-356. J Ind Microbiol **7:**77–88. http://dx.doi.org/10.1007/BF01576069.
12. **Suske WA, van Berkel WJH, Kohler HPE.** 1999. Catalytic mechanism of 2-hydroxybiphenyl 3-monooxygenase, a flavoprotein from *Pseudomonas azelaica* HBP1. J Biol Chem **274:**33355–33365. http://dx.doi.org/10.1074/jbc.274.47.33355.
13. **Pham TTM, Tu Y, Sylvestre M.** 2012. Remarkable ability of *Pandoraea pnomenusa* B356 biphenyl dioxygenase to metabolize simple flavonoids. Appl Environ Microbiol **78:**3560–3570. http://dx.doi.org/10.1128/AEM.00225-12.
14. **Seeger M, Gonzalez M, Camara B, Munoz L, Ponce E, Mejias L, Mascayano C, Vasquez Y, Sepulveda-Boza S.** 2003. Biotransformation of natural and synthetic isoflavonoids by two recombinant microbial enzymes. Appl Environ Microbiol **69:**5045–5050. http://dx.doi.org/10.1128/AEM.69.9.5045-5050.2003.
15. **Shindo K, Nakamura R, Osawa A, Kagami O, Kanoh K, Furukawa K, Misawa N.** 2005. Biocatalytic synthesis of monocyclic arene-dihydrodiols and -diols by *Escherichia coli* cells expressing hybrid toluene/biphenyl dioxygenase and dihydrodiol dehydrogenase genes. J Mol Catal B Enzym **35:**134–141. http://dx.doi.org/10.1016/j.molcatb.2005.06.010.
16. **Tehrani R, Lyv MM, Kaveh R, Schnoor JL, Van Aken B.** 2012. Biodegradation of mono-hydroxylated PCBs by *Burkholderia xenovorans*. Biotechnol Lett **34:**2247–2252. http://dx.doi.org/10.1007/s10529-012-1037-x.
17. **Colbert CL, Agar NY, Kumar P, Chakko MN, Sinha SC, Powlowski JB, Eltis LD, Bolin JT.** 2013. Structural characterization of *Pandoraea pnomenusa* B-356 biphenyl dioxygenase reveals features of potent polychlorinated biphenyl-degrading enzymes. PLoS One **8:**e52550. http://dx.doi.org/10.1371/journal.pone.0052550.
18. **Kumar P, Mohammadi M, Viger JF, Barriault D, Gomez-Gil L, Eltis LD, Bolin JT, Sylvestre M.** 2011. Structural insight into the expanded PCB-degrading abilities of a biphenyl dioxygenase obtained by directed evolution. J Mol Biol **405:**531–547. http://dx.doi.org/10.1016/j.jmb.2010.11.009.
19. **Gomez-Gil L, Kumar P, Barriault D, Bolin JT, Sylvestre M, Eltis LD.** 2007. Characterization of biphenyl dioxygenase of *Pandoraea pnomenusa* B-356 as a potent polychlorinated biphenyl-degrading enzyme. J Bacteriol **189:**5705–5715. http://dx.doi.org/10.1128/JB.01476-06.
20. **Pham TT, Sylvestre M.** 2013. Has the bacterial biphenyl catabolic pathway evolved primarily to degrade biphenyl? The diphenylmethane case. J Bacteriol **195:**3563–3574. http://dx.doi.org/10.1128/JB.00161-13.
21. **Standfuß-Gabisch C, Al-Halbouni D, Hofer B.** 2012. Characterization of biphenyl dioxygenase sequences and activities encoded by the metagenomes of highly polychlorobiphenyl-contaminated soils. Appl Environ Microbiol **78:**2706–2715. http://dx.doi.org/10.1128/AEM.07381-11.
22. **Kucerova P, Mackova M, Chroma L, Burkhard J, Triska J, Demnerova K, Macek T.** 2000. Metabolism of polychlorinated biphenyls by *Solanum nigrum* hairy rootclone SNC-90 and analysis of transformation products. Plant Soil **225:**109–115. http://dx.doi.org/10.1023/A:1026551728196.
23. **Singh H.** 2006. Mycoremediation: fungal bioremediation. John Wiley & Sons, Inc, Hoboken, NJ.
24. **Nishihara Y.** 1988. Comparative toxicity of 4-chlorobiphenyl and its metabolite 4-chloro-4′-biphenylol in isolated rat liver mitochondria. Biochem Pharmacol **37:**2915–2926. http://dx.doi.org/10.1016/0006-2952(88)90276-6.
25. **Connor K, Ramamoorthy K, Moore M, Mustain M, Chen I, Safe S, Zacharewski T, Gillesby B, Joyeux A, Balaguer P.** 1997. Hydroxylated polychlorinated biphenyls (PCBs) as estrogens and antiestrogens: structure-activity relationships. Toxicol Appl Pharmacol **145:**111–123. http://dx.doi.org/10.1006/taap.1997.8169.
26. **Barriault D, Plante MM, Sylvestre M.** 2002. Family shuffling of a targeted *bphA* region to engineer biphenyl dioxygenase. J Bacteriol **184:**3794–3800. http://dx.doi.org/10.1128/JB.184.14.3794-3800.2002.
27. **Vézina J, Barriault D, Sylvestre M.** 2008. Diversity of the C-terminal portion of the biphenyl dioxygenase large subunit. J Mol Microbiol Biotechnol **15:**139–151. http://dx.doi.org/10.1159/000121326.
28. **Sambrook J, Fritsch EF, Maniatis T.** 1989. Molecular cloning: a laboratory manual, 2nd ed. Cold Spring Harbor Laboratory Press, Cold Spring Harbor, NY.
29. **Sylvestre M.** 1980. Isolation method for bacterial isolates capable of growth on *p*-chlorobiphenyl. Appl Environ Microbiol **39:**1223–1224.
30. **Toussaint JP, Pham TTM, Barriault D, Sylvestre M.** 2012. Plant exudates promote PCB degradation by a rhodococcal rhizobacteria. Appl Microbiol Biotechnol **95:**1589–1603. http://dx.doi.org/10.1007/s00253-011-3824-z.
31. **Mohammadi M, Viger JF, Kumar P, Barriault D, Bolin JT, Sylvestre M.** 2011. Retuning Rieske-type oxygenases to expand substrate range. J Biol Chem **286:**27612–27621. http://dx.doi.org/10.1074/jbc.M111.255174.
32. **Hurtubise Y, Barriault D, Sylvestre M.** 1996. Characterization of active recombinant His-tagged oxygenase component of *Comamonas testosteroni* B-356 biphenyl dioxygenase. J Biol Chem **271:**8152–8156. http://dx.doi.org/10.1074/jbc.271.14.8152.
33. **Morris GM, Huey R, Lindstrom W, Sanner MF, Belew RK, Goodsell DS, Olson AJ.** 2009. AutoDock4 and AutoDockTools4: automated docking with selective receptor flexibility. J Comput Chem **30:**2785–2791. http://dx.doi.org/10.1002/jcc.21256.
34. **Massé R, Messier F, Ayotte C, Lévesque M-F, Sylvestre M.** 1989. A comprehensive gas chromatographic/mass spectrometric analysis of 4-chlorobiphenyl bacterial degradation products. Biomed Environ Mass Spectrom **18:**27–47. http://dx.doi.org/10.1002/bms.1200180106.
35. **McLean MR, Bauer U, Amaro AR, Robertson LW.** 1996. Identification of catechol and hydroquinone metabolites of 4-monochlorobiphenyl. Chem Res Toxicol **9:**158–164. http://dx.doi.org/10.1021/tx950083a.
36. **Barriault D, Durand J, Maaroufi H, Eltis LD, Sylvestre M.** 1998. Degradation of polychlorinated biphenyl metabolites by naphthalene-catabolizing enzymes. Appl Environ Microbiol **64:**4637–4642.
37. **Karplus M.** 1963. Vicinal poton coupling in nuclear magnetic resonance. J Am Chem Soc **85:**2870–2871. http://dx.doi.org/10.1021/ja00901a059.
38. **L'Abbée JB, Tu YB, Barriault D, Sylvestre M.** 2011. Insight into the metabolism of 1,1,1-trichloro-2,2-bis(4-chlorophenyl)ethane (DDT) by biphenyl dioxygenases. Arch Biochem Biophys **516:**35–44. http://dx.doi.org/10.1016/j.abb.2011.09.016.
39. **Sondossi M, Lloyd BA, Barriault D, Sylvestre M, Simard M.** 1995. Microbial transformation of a dihydroxybiphenyl. Acta Crystallogr C **51:**491–494. http://dx.doi.org/10.1107/S0108270194008590.
40. **Ahmad D, Sylvestre M, Sondossi M.** 1991. Subcloning of *bph* genes from *Pseudomonas testosteroni* B-356 in *Pseudomonas putida* and *Escherichia coli*: evidence for dehalogenation during initial attack on chlorobiphenyls. Appl Environ Microbiol **57:**2880–2887.
41. **Barriault D, Lépine F, Mohammadi M, Milot S, Leberre N, Sylvestre M.** 2004. Revisiting the regiospecificity of *Burkholderia xenovorans* LB400 biphenyl dioxygenase toward 2,2′-dichlorobiphenyl and 2,3,2′,3′-tetrachlorobiphenyl. J Biol Chem **279:**47489–47496. http://dx.doi.org/10.1074/jbc.M406808200.
42. **Kumamaru T, Suenaga H, Mitsuoka M, Watanabe T, Furukawa K.** 1998. Enhanced degradation of polychlorinated biphenyls by directed evolution of biphenyl dioxygenase. Nat Biotechnol **16:**663–666. http://dx.doi.org/10.1038/nbt0798-663.
43. **Suenaga H, Nishi A, Watanabe T, Sakai M, Furukawa K.** 1999. Engineering a hybrid pseudomonad to acquire 3,4-dioxygenase activity for

polychlorinated biphenyls. J Biosci Bioeng **87:**430–435. http://dx.doi.org/10.1016/S1389-1723(99)80090-5.
44. **Barriault D, Sylvestre M.** 2004. Evolution of the biphenyl dioxygenase BphA from *Burkholderia xenovorans* LB400 by random mutagenesis of multiple sites in region III. J Biol Chem **279:**47480–47488. http://dx.doi.org/10.1074/jbc.M406805200.
45. **Kumar P, Mohammadi M, Dhindwal S, Pham TT, Bolin JT, Sylvestre M.** 2012. Structural insights into the metabolism of 2-chlorodibenzofuran by an evolved biphenyl dioxygenase. Biochem Biophys Res Commun **421:**757–762. http://dx.doi.org/10.1016/j.bbrc.2012.04.078.
46. **Seo J, Kang SI, Won D, Kim M, Ryu JY, Kang SW, Um BH, Pan CH, Ahn JH, Chong Y, Kanaly RA, Han J, Hur HG.** 2011. Absolute configuration-dependent epoxide formation from isoflavan-4-ol stereoisomers by biphenyl dioxygenase of *Pseudomonas pseudoalcaligenes* strain KF707. Appl Microbiol Biotechnol **89:**1773–1782. http://dx.doi.org/10.1007/s00253-010-2989-1.
47. **Lee K, Gibson DT.** 1996. Toluene and ethylbenzene oxidation by purified naphthalene dioxygenase from *Pseudomonas* sp. strain NCIB 9816-4. Appl Environ Microbiol **62:**3101–3106.
48. **Safe SH.** 1994. Polychlorinated biphenyls (PCBs)—environmental impact, biochemical and toxic responses, and implications for risk assessment. Crit Rev Toxicol **24:**87–149. http://dx.doi.org/10.3109/10408449409049308.